

Horizontal Tail Maneuver Load Predictions Using Backpropagation Neural Networks

David Kim* and Maciej Marciniak†

Embry-Riddle Aeronautical University, Daytona Beach, Florida 32114-3900

A backpropagation neural network was used to predict maneuver-induced strains in the horizontal tail spar of a small aircraft transport. Linear accelerometer, angular accelerometer, rate gyro, and strain gauge signals were recorded during flights for Dutch-roll, roll, sideslip, level-turn, and push-pull maneuvers. Sensor signals were filtered and used to train the network. The strains in the horizontal tail spar were predicted successfully to within $50\ \mu\epsilon$ of their strain gauge values resulting in a significant improvement over the traditional regression analysis predictions. This method can be used to establish the horizontal tail load spectra of airplanes already in service, where installation of strain gauges is impractical.

Introduction

FEDERAL aviation regulations require that structures critical to the safe operation of an aircraft must not fail within their expected lifetimes due to damage caused by the repeated loads typical to its operations. This requirement generates the need for evaluation of fatigue life of the critical aircraft structures. Two of these are the wings and the empennage structures. Most commonly, the fatigue life is determined using the Palmgren–Miner linear cumulative damage theory. To calculate the fatigue life using this method, one must know the loading history or spectra of the aircraft. There is information on flight loads, that is, normal acceleration near aircraft center of gravity (CG Nz), for general aviation aircraft that can be used to determine the fatigue life of airplane wings. However, there is no comparable information for empennage loads.

Clearly, to compile these data, an efficient, practical, and cost-effective method of monitoring empennage loads is much needed. If it is to be widely adopted as a flight loads-monitoring tool for small aircraft transport, the unit price must be low enough to attract the interest of small aircraft fleet operators and owners. In addition, if a useful flight load database is to be created, a large, comprehensive number of aircraft flown in a variety of flight conditions, and missions will have to be monitored. This suggests that the best system for the task is one that is easy and inexpensive to install and maintain similar to the NASA VGH (velocity, load factor, altitude) recorder¹ but one that is more robust and versatile that is also capable of accurately predicting loads in empennage structure.

Currently, in the absence of better data, the normal acceleration spectra developed from the NASA VGH study is being used to determine fatigue loads on empennage structures. However, previous work by the author showed that there is only a weak correlation (less than 0.3) between these normal accelerations and the strains in the horizontal tail. Thus, the primary focus of the present research is to find some other method of relating data collected near the aircraft CG to strains occurring elsewhere, specifically, in the aircraft horizontal tail.

Because the cost of many small aircraft transports cannot justify expensive load-monitoring systems, it is important that the method

works with a minimal set of instrumentation appropriate for low-cost general aviation aircraft operators and owners. Similar to the NASA VGH study, this method can then be used to establish the horizontal tail load spectra of airplanes already in service, where installation of strain gauges is impractical. Furthermore, flight data collected could be used to build a more appropriate database of empennage fatigue-load spectra and, together with the existing fatigue load data for the wings, could be used to design much safer next generation of airplanes.

Previous Work

NASA VGH program was the largest and the longest running in-flight load-monitoring program for general aviation aircraft. In the United States, it also represents the only comprehensive general aviation flight loads-monitoring program. This program started in the early 1960s and continued until 1982. During that time, 42,155 h of data were collected on 105 airplanes. Airplanes were chosen from nine usage groups: twin-engine executive, single-engine executive, personal, instructional, commercial survey, aerial applications (fire fighting, etc.), aerobatic, commercial, and float operations. Data for 35,286 h of operation from 95 airplanes were evaluated and presented as a part of a fatigue evaluation method for wings in Ref. 2. The final report on the VGH project, Ref. 1 was published in 1993. As the original NASA VGH program focused on normal accelerations, the need for a similar program to evaluate fatigue life of vertical aerodynamic surfaces such as fins, rudders, and winglets was expressed by the authors of that report. Since only the accelerations near the CG were measured, this project left the problem of empennage structure fatigue loads unaddressed.

More recently, The Netherlands has conducted an extensive flight loads programs. Cooperation between the Dutch National Aerospace Laboratory, the Dutch national airlines KLM, and the Fokker company resulted in a yearlong in-flight tail loads-monitoring program.³ In this program, strain surveys were performed on the tail of a Fokker 100 airliner. Data were collected over a period of one year of commercial service. Large amounts of data were collected, but for a large fleet of aircraft, the method used, direct measurement using strain gauges, is not considered to be a viable approach due to the cost of installation and maintenance.

There were also some works done in the area of predictions of flight loads. Research done by the U.S. Navy has successfully demonstrated that it is possible to predict strains at some point of the structure from the flight parameter data collected at another point. In this case, CG Nz, wing sweep angle, angle of attack, roll rate, Mach number, altitude, weight-on-wheels indicator, and an indicator for takeoff, landing, and peak-or-valley data were used to predict strain at a point on aft fuselage of an F-14B aircraft. Correlation coefficients of 0.93–0.97 were achieved between the predicted strains and the measured strains.⁴ Another research effort by the

Received 30 April 2001; revision received 6 July 2001; accepted for publication 11 November 2001. Copyright © 2001 by the American Institute of Aeronautics and Astronautics, Inc. All rights reserved. Copies of this paper may be made for personal or internal use, on condition that the copier pay the \$10.00 per-copy fee to the Copyright Clearance Center, Inc., 222 Rosewood Drive, Danvers, MA 01923; include the code 0021-8669/02 \$10.00 in correspondence with the CCC.

*Professor, Department of Aerospace Engineering. Senior Member AIAA.

†Graduate Student, Department of Aerospace Engineering; currently Lead Engineer, 737 Thrust Reverses Stress Engineer, The Boeing Aircraft Company, Wichita, Kansas, 67277.

U.S. Navy has successfully employed neural networks to predict loads experienced in-flight by the main rotor blades of a helicopter. Neural networks were chosen because of the difficulties associated with attempts to measure directly loads in a rotating system. The inputs to the network were load factor, longitudinal, lateral, pitch, roll, and yaw accelerations, airspeed, aircraft mass, rate of climb, rotor speed, rotor control servo position, and stabilator position. Correlation coefficients of 0.93–0.96 were achieved between the predicted and the actual loads.⁵

Similar work was accomplished at Virginia Polytechnic Institute and State University using neural networks to predict the time-varying mean and oscillatory components of the tailboom bending loads and the pitch link loads. For this application, the input variables were pitch rate, roll rate, yaw rate, vertical acceleration, lateral acceleration, longitudinal acceleration, longitudinal control position, and lateral control position. Correlation coefficients of 0.907–0.977 between the predicted and actual loads were achieved.⁶ At Embry-Riddle Aeronautical University, Kim and Marciniak applied the backpropagation neural networks technique to the prediction of vertical tail maneuver loads for general aviation airplanes.⁷ In this work, a minimum set of sensors was also identified that is necessary for the prediction of the strains in the vertical tail of a small transport airplane.

Current Work

Despite that previous studies using multiple regression analysis showed only a small correlation between accelerations measured near the aircraft CG and the corresponding strains in the empennage structure, it is not unreasonable to expect that there, nevertheless, is a relationship, probably nonlinear, between these quantities. The purpose of this research is to employ artificial neural networks as a means of defining such a relationship. Neural networks are capable of modeling nonlinear relationships between variables and offer a good chance of finding the solution. Regression analysis performed poorly mainly due to two reasons. First, there is a phase lag between horizontal tail load and sensor measurement. Second, the phase lag is dependent on maneuver performed. For a prediction method to be useful, one must be able to predict the loads without a priori knowledge of maneuvers performed.

The work also concentrates on finding the minimum set of instrumentation sensors needed to predict accurately horizontal tail strains, the minimum threshold value of significant strains, and the correlation between sensor output and the empennage flight loads. For small transport airplanes, the cost and ease of installation of the loads-monitoring system is a major issue. The testbed aircraft was a Cessna 172P. For many of these airplanes, even a cost of U.S. \$2000 borders on being excessive. The inputs to the neural networks were provided by signals collected in-flight from three angular accelerometers, three rate gyros, two linear accelerometers near the aircraft CG, and two linear accelerometers in the tail cone. In addition, the aircraft had sensors for airspeed, pressure altitude, angle of attack, and sideslip measurements as well as strain gauges on aircraft primary structures.

Neural Networks Background

Artificial neural networks are information processing systems that attempt to emulate some of the processing characteristics of the human brain. Much like its biological counterpart, an artificial neural network consists of a large number of heavily interconnected simple processing elements. This brainlike organization gives the neural network parallel processing and learning capability. Most neural networks, like the human brain, require iterative feedback training. Depending on the task, either supervised or unsupervised training is needed. Supervised training means that the neural network is given a set of input-correct output pairs to train on. Unsupervised training means that the network is only given the input data to train on. In general, prediction requires supervised training. Neural networks are often viewed as black boxes because, whereas neural networks have definite mathematical expressions that define them, they are not normally represented in explicit mathematical form due to their complexity. This is especially true for the complex networks that

may consist of hundreds of processing elements and thousands of connections. Also, finding the right arrangement of processing elements for a given problem usually involves significant amounts of trial and error because there is no systematic method available presently for determining this information a priori.

Selection of the proper network architecture for the task is not an exact science. As a rule, the neural network architecture is such that the input layer has a number of neurons equal to the number of the input variables. In case of a prediction problem, the number of neurons in the output layer must be equal to the number of predicted variables. In the case of a classification problem, the number of neurons in the output layer must be equal to the number of possible classifications. The number of neurons needed in the hidden layer is more difficult to establish. An arbitrary number of neurons in the hidden layer is chosen to start with. The optimum number of neurons is then found by adding or subtracting a few neurons at a time and retraining the net. Typically, there is a number of hidden layer neurons that results in the best network performance.

Experimental Apparatus

A Cessna 172P was used to collect the flight loads data. Figure 1 shows the locations of the sensors and the data acquisition system in the aircraft. Two Columbia Research Model 2681 strain sensors were located on the front spar of the left horizontal stabilizer. These strain sensors are temperature compensated to account for the changes in temperature expected with altitude and have maximum error of $60 \mu\epsilon$. Two Columbia Research SA-107BHP linear accelerometers were mounted to the tailcone bulkhead to provide linear accelerations of the empennage. One of these was mounted with its sensing axis aligned along the aircraft y axis (positive starboard) and the other along the aircraft z axis (positive downward). The remaining two linear accelerometers (same type) were located in the cabin of the aircraft to provide linear accelerations of the aircraft CG. These accelerometers were installed similarly to the ones in the tailcone: one along the aircraft y axis and one along the aircraft z axis.

Three Murata Gyrostar ENV-05H-02 solid-state rate gyros and three Shaevitz angular accelerometers were installed in the baggage compartment on a removable instrument pallet. One rate gyro and one angular accelerometer were provided for each of the aircraft major axes: x (roll), y (pitch), and z (yaw). The rate gyros and

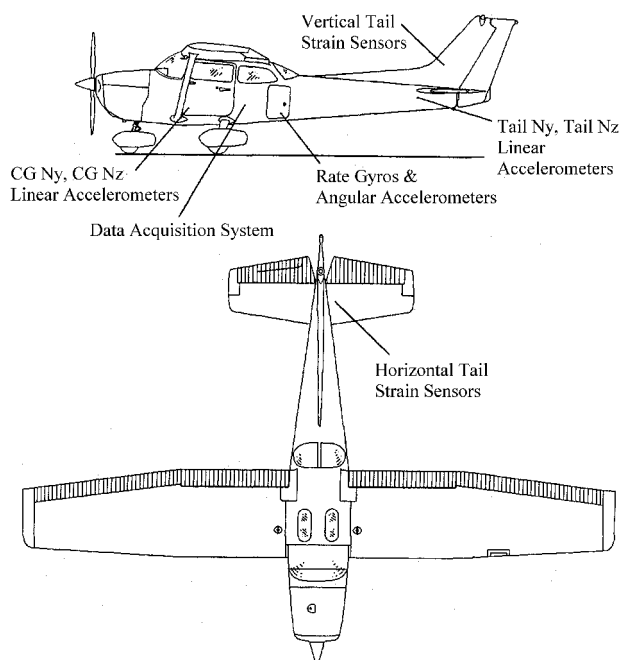


Fig. 1 Location of sensors and data acquisition system.

the angular accelerometers were added to provide a more direct measurement of the desired kinematic variables because previous investigation by the authors showed that exclusive use of the linear accelerometers was not sufficient to predict the empennage flight loads of a small aircraft with the desired accuracy.

Signals from the sensors were collected by an IOTech DaqBook 216 portable data acquisition system. This is a 16-bit digital data acquisition system capable of handling up to 256 input channels at 100 kHz. For this work, 200 Hz was the sampling rate used. The DaqBook 216 was equipped with an IOTech DBK 15 universal current/voltage input card and an IOTech DBK43 strain gauge module. The DBK 15 card was used to collect the linear accelerometer, rate gyro, and the angular accelerometer signals, whereas the DBK 43 card collected data from the strain gauges. A portable computer was used to record the data during flight.

Because of practical considerations limiting the tracking of aircraft takeoff weight and CG location for small transport airplanes in fleet operations, these parameters were not considered with expected loss of some accuracy. Airspeeds were recorded but not used as an input parameter due to position error effects associated with the static pressure port installation of this aircraft. The Cessna 172 has a single static pressure source on the port side of the fuselage just forward of the pilot's door. The resulting large airspeed error during sideslip conditions makes its measurements of limited value if this method is to be used on fleet airplanes.

Testing Procedure

The data were acquired in-flight from a series of maneuvers performed at 3000 ft. Flight conditions for all of the flights were smooth. The baseline was chosen as 1 g level flight condition, and the strain sensors were adjusted to provide 0.0 Volts for this condition. Sensor outputs were recorded for sideslip, level turn, roll, Dutch-roll, and push-pull maneuvers. Each maneuver was performed at 65, 80, and 95 knots indicated airspeed (KIAS). A maximum load factor of 3.0 was reached during the push-pull maneuver. The maneuvers and the speeds at which they were performed were chosen to cover the full range of aircraft motion under normal flight conditions and a sizable portion of its flight envelope. Negative load factors were avoided during push-pull maneuvers because it is very unlikely for this airplane type to experience negative gravitational acceleration during normal operations. The part of the flight envelope that was covered is shown in Fig. 2 and was judged sufficient for establishing a method of strain prediction.

Two data sets were recorded, one intended for the training of the neural networks and one for the testing. These two data sets were recorded on different days to provide differing flight conditions. In addition, a separate file containing a typical flight profile that may be encountered by an aircraft was recorded. This file contained a climb simulating the initial climb after takeoff, a variety of turns, altitude changes, and velocity changes performed in a random order and at a wide range of airspeeds, as well as a descent with airspeed decrease simulating an approach to a landing. This file was recorded to evaluate how well the neural networks would generalize from the

carefully staged training data to data that may be collected during a typical flight.

Postprocessing

Preliminary neural network results indicated that the prediction accuracy improved when the raw data were filtered before training the network. A frequency spectrum analysis was performed using DADisp 4.0. It indicated that the signals resulting from the pilot control inputs had frequencies less than 1.5 Hz. A low-pass filter with a 2-Hz cutoff frequency was used to filter the data for maneuver loads.

Selection of Neural Network

The signals that were used for the prediction of strains in the horizontal tail were CG Nz, Tail Nz, pitch rate, roll rate, yaw rate, pitch acceleration, roll acceleration, and yaw acceleration. For the neural networks to learn properly the relationship between the strains and the kinematic variables, the full range of measured strains had to be represented within the training files. Maximum strains in the horizontal tail occurred during roll and Dutch-roll maneuvers and not during the symmetric pitching or yawing maneuver as is commonly believed.

The choice of a neural network type was driven by the fact that the relationship between the kinematic variables and the strain was unknown and that there was no guarantee that this relationship remained constant throughout the test flight envelope. A modular neural network (MNN) was chosen to handle this problem. An MNN may be thought of as a generalization of a backpropagation neural network. It consists of group of neural networks, referred to as local experts, competing to learn different aspects of a problem. A gating network controls the competition and learns to assign different regions of the data space to different local expert network. Thus, if the relationship between the strain and kinematic variables changed from one maneuver to another or from one speed to another, the neural network would still be able to learn to predict the strains regardless of flight conditions.

Both the gating network and local experts have full connections from the input layer. The gating network has as many output nodes as there are local experts. Training occurs simultaneously for the gating network and for local experts. Competition among local experts is encouraged, so that, for a given input vector, the gating network will tend to choose a single local expert rather than a mixture of them. In this way, the input space is automatically partitioned into regions and each local expert takes responsibility for a different region.

Neural Network Implementation

The neural networks created in this research were formed, trained, and tested using the NeuralWorks Professional II+ version 5.20 software. This program is capable of automatically generating an MNN from the specified parameters.⁸ The parameters of the networks selected are listed in Table 1.

Because one of the objectives was to determine the minimum set of sensors, the number of input layer neurons was varied from 2 to 6 as various combinations of inputs were tried out. Whereas different numbers of hidden layers were tested, the final network had

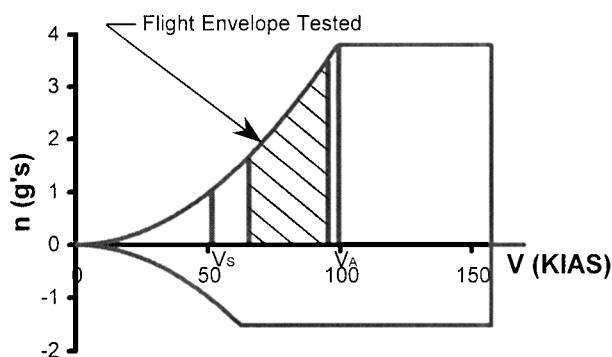


Fig. 2 Approximate flight envelope covered.

Table 1 Parameters of the MNN

Inputs	Dependent on the combination of signals used for input
Local expert hidden layer neurons	30
Local expert output layer neurons	1
Gating network hidden layer neurons	400
Gating network output layer neurons	5
Learning rule	EDBD
Transfer function	TANH
Epoch	15
F' offset	0.3

two hidden layers. The number of neurons in the hidden layer of each local expert was arbitrarily set to 30. During initial testing, this number was increased to as high as 50 with no appreciable change in network performance. All local experts had a single neuron in their output layer. This was dictated by the fact that each of these networks was expected to predict a single value, the strain in the horizontal tail.

The number of neurons in the hidden layer of the gating network was set to 400. Gating networks with less than 400 hidden layer neurons were tried, but the network performance decreased substantially. The number of the neurons in the output layer of the gating network (and subsequently the number of the local experts) was set to five. This proved sufficient as none of the subsequently trained networks required the use of more than three of the five available local experts.

The extended delta-bar-delta (EDBD) learning rule was selected. This learning rule automatically selects and adjusts the learning coefficient, the learning coefficient ratio, the learning coefficient transition point, and the momentum term. This minimized the learning time and reduced the number of network parameters that had to be selected iteratively. A hyperbolic tangent transfer function (TANH) was appropriate for the problem at hand because the input values ranged from -1 to $+1$. The epoch sets the number of training pairs that are presented to the network before the weights are updated. Larger and smaller epochs were tried for both networks but resulted in generally worsened network performance. The F' offset is a constant added to the value of the derivative of the neuron activation function during training to prevent neuron saturation. The Neural-Works users guide suggests that it be set to 0.3 for a TANH activation function. F' offsets of 0.1 and 0.2 were also tried with no change in the results. With a 100-MHz Pentium personal computer, the analysis was a slow process with only three network training runs performed per day.

Results

Before the results can be evaluated, one must first establish a baseline definition of the ideal neural network output. First, not all stresses that may be experienced by a structure contribute signifi-

cantly to the accumulated fatigue damage. A stress lower than that necessary to cause failure after 10^7 cycles (for a given stress ratio) is not considered causing fatigue damage. According to the S-N curves for 2024 aluminum, the minimum stress that causes fatigue damage is 5000 psi (34.5 MPa) for a full stress reversal. Thus, an insignificant stress region was defined to exist at or below 1000 psi (6.9 MPa). Second, within the significant stress region, a tolerance band of $\pm 50 \mu\epsilon$ was assumed, as compared to the maximum error for the strain sensors of $60 \mu\epsilon$. Because eventually this method is to be used to evaluate the fatigue life of empennage structures, the stresses should be predicted at least as accurately as they are plotted on the maximum stress axis of the S-N curves. The stresses in the S-N curves found in Ref. 9 are plotted to within 1000 psi (6.9 MPa), which for aluminum translates to $100 \mu\epsilon$. Thus, this number was selected as the full width of the tolerance band.

Table 2 shows the strain increments measured in-flight for each maneuver. Maximum strain increments in the horizontal tail occurred during Dutch-roll and roll maneuvers. Only a small fraction of the recorded strain increments due to maneuver loads resulted in stresses outside the insignificant region. It was surprising that the steady-state maneuvers such as the level turn resulted in small strains. The horizontal tail strains observed during push-pulls were also surprisingly smaller than expected, though not as small as those resulting from the stabilized g turn maneuvers.

The best horizontal tail strain prediction results were obtained when the x , y , and z axes angular accelerometers and the CG Nz linear accelerometer signals from Dutch-roll at 80 KIAS, roll at 80 KIAS, and push-pull at 80 KIAS were used to train the neural network. These results are summarized in Table 3 and Figs. 3–12 for the two maneuvers that induced the highest strain increments, Dutch-roll and roll. Table 3 shows the number of significant strains, number of strains predicted that fell outside of the tolerance band, and the maximum error of prediction for those maneuvers that caused at least some significant stresses in the horizontal tail. Figures 3–12 present the results as XY plots of predicted strains vs measured strains. Because the neural networks software required that the parameters range from -1 to $+1$, the strains were normalized to a predetermined maximum value for convenience.

Only a small fraction of the recorded strain increments due to maneuver loads resulted in stresses greater than 1000 psi (6.9 MPa). Out of 232,040 records collected, only 4332 or about 2% contained strains that produced significant horizontal tail stresses. The neural network was able to predict 93% of the significant strains to within $50 \mu\epsilon$ of their corresponding measured values. It had a tendency to underestimate the magnitudes of strains resulting from the Dutch-roll maneuvers, as is apparent from Figs. 3–12. The strain prediction for the roll maneuver produced better results when the strain gauge was in tension, positive normalized strain. In this region, the predicted strains agreed closely with the measured strains. When the strain gauge was in compression, negative normalized strain, as the strains increased, the neural network again tended to underestimate the strains.

Table 2 Maximum and minimum strain increments observed for each maneuver

Maneuver	Maximum strain $\mu\epsilon$	Minimum strain $\mu\epsilon$
Dutch roll	112	-131
Roll	95	-160
Sideslip left	26	-98
Sideslip right	82	-59
Stabilized g turn left	17	-63
Stabilized g turn right	32	-67
Push-Pull	44	-97

Table 3 Summary of horizontal tail strain prediction results

Maneuver	Significant stress region			Entire data set		
	Records	Records outside tolerance band	Maximum error of prediction $\mu\epsilon$	Records	Records outside tolerance band	Maximum error of prediction $\mu\epsilon$
Dutch roll, 80 KIAS, training set	384	0	45	5,801	0	49
Dutch roll, 80 KIAS, testing set	45	0	36	5,801	102 (2%)	58
Dutch roll, 95 KIAS, training set	184	0	32	5,801	357 (6%)	69
Dutch roll, 95 KIAS, testing set	730	202 (27%)	82	5,801	604 (10%)	82
Roll, 65 KIAS, training set	313	0	30	5,801	0	40
Roll, 65 KIAS, testing set	25	0	38	5,801	0	42
Roll, 80 KIAS, training set	585	0	44	5,801	0	44
Roll, 80 KIAS, testing set	297	0	39	5,801	58 (1%)	55
Roll, 95 KIAS, training set	1,021	34 (3%)	55	5,801	103 (2%)	66
Roll, 95 KIAS, testing set	748	54 (7%)	59	5,801	236 (4%)	63
Others	0	—	—	169,698	—	—
Total	4,332	290 (7%)	—	232,040	16,950 (7%)	—

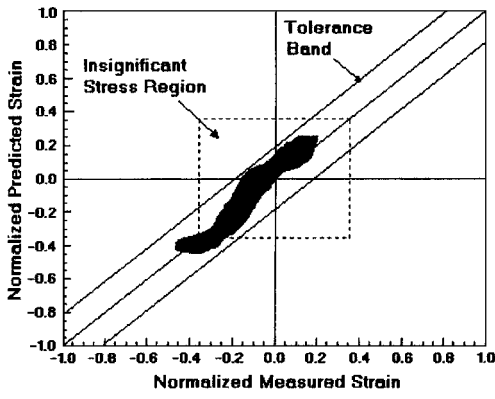
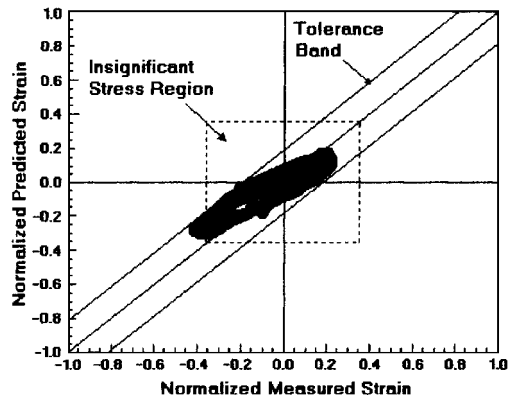


Fig. 3 Dutch-roll, 80 KIAS, horizontal tail, training set: strain prediction results.

Fig. 7 Roll, 65 KIAS, horizontal tail, training set: strain prediction results.

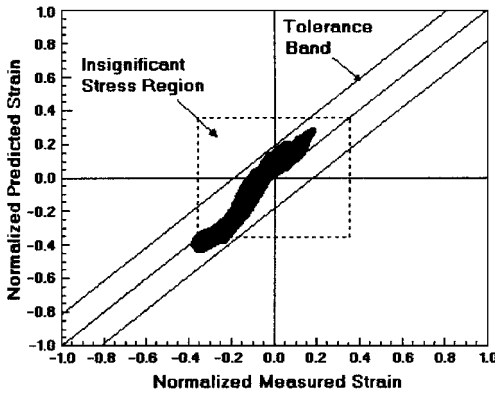
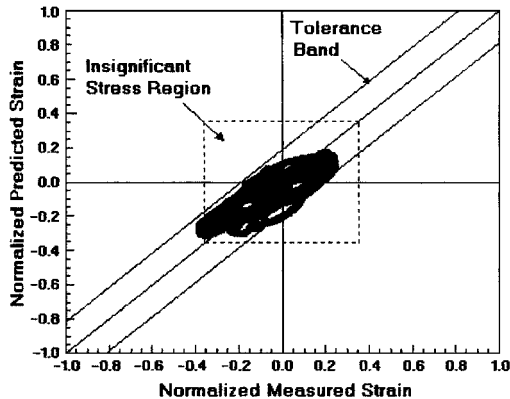


Fig. 4 Dutch-roll, 80 KIAS, horizontal tail, testing set: strain prediction results.

Fig. 8 Roll, 65 KIAS, horizontal tail, testing set: strain prediction results.

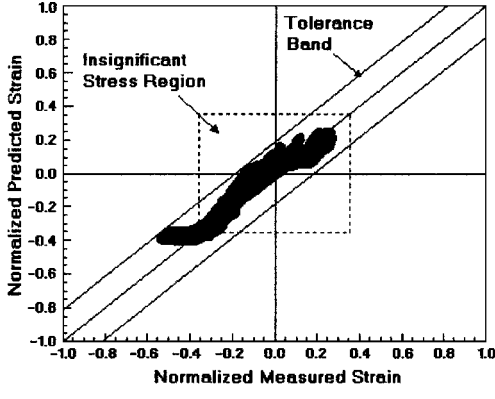
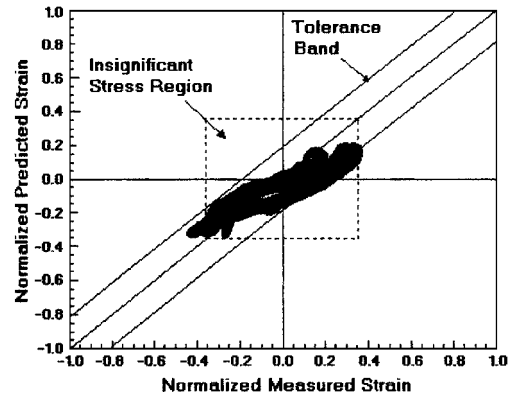


Fig. 5 Dutch-roll, 95 KIAS, horizontal tail, training set: strain prediction results.

Fig. 9 Roll, 80 KIAS, horizontal tail, training set: strain prediction results.

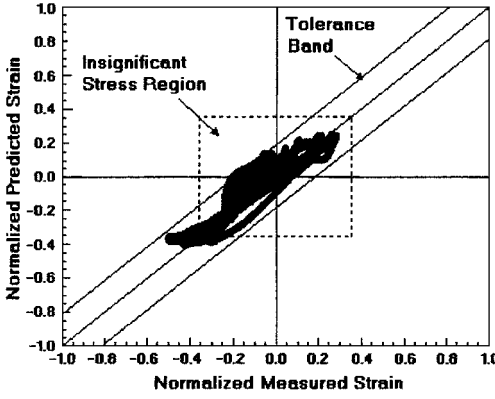
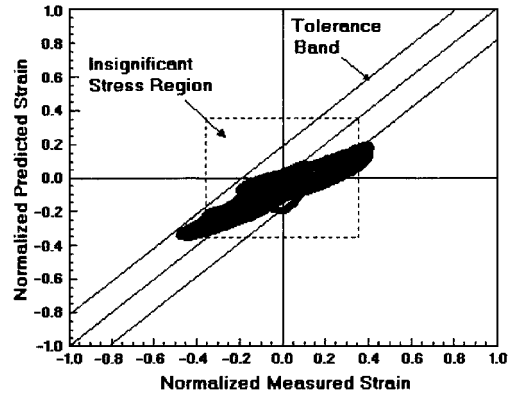


Fig. 6 Dutch-roll, 95 KIAS, horizontal tail, testing set: strain prediction results.

Fig. 10 Roll, 80 KIAS, horizontal tail, testing set: strain prediction results.

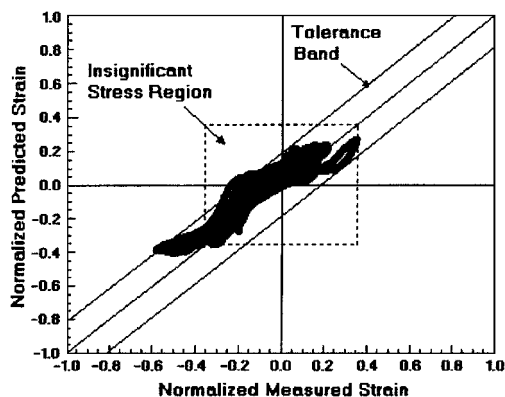


Fig. 11 Roll, 95 KIAS, horizontal tail, training set: strain prediction results.

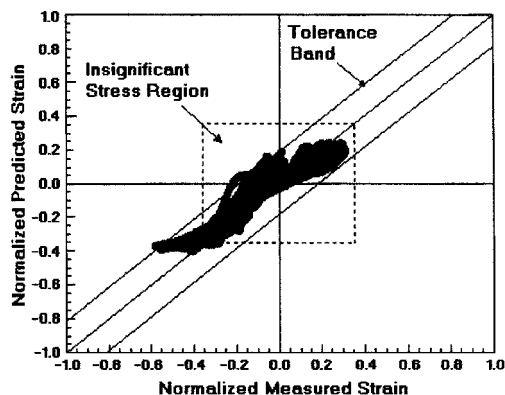


Fig. 12 Roll, 95 KIAS, horizontal tail, testing set: strain prediction results.

Conclusions

To within acceptable limits, the backpropagation neural networks successfully predicted most of the strain behavior that resulted from the maneuver loads in the horizontal tail structure of the Cessna 172P. The x -, y -, and z -axis angular accelerometer and CG Nz linear accelerometer signals were needed to train the neural networks that were used to predict the strains resulting from the maneuver loads. These sensors appear to be the minimum set of sensors required to predict the strains in the horizontal tail of the airplane. Although not as accurate as direct measurement using strain gauges, the remote sensors and the neural networks technique seem adequate for flight load analysis to establish the fatigue loads spectra database. The appearance of asymptotic behavior observed in roll predictions raises interest for future research, but in the case of this testbed airplane, the prediction results are still valid because the airplane should not

experience loads much greater than those measured under normal and proper operations. The design maneuvering speed is 99 KIAS, only 4 KIAS higher than the test point. Full and abrupt control deflection maneuvers at speeds greater than the design maneuvering speed is not recommended. Once the neural network has been developed for a particular airplane instrumented with strain gauges, this method can be used for a fleet of same model airplanes to establish the horizontal tail load spectra of airplanes already in-service where installation of strain gauges is impractical.

The neural networks utilized the angular accelerometer signals. Present day angular accelerometers of the type used cost between \$1700 and \$3000. To reduce the price of the instrumentation, the rate gyro signals were also numerically differentiated to obtain angular accelerations. These derived angular acceleration signals or perhaps the rate gyro signals should be tried instead of the raw angular accelerations to train the neural networks. The neural networks developed for the horizontal tail may be optimized to reduce the amount of time necessary to calculate the strains and, if necessary, to improve the accuracy of the prediction. Finally, the method of strain prediction developed herein should be verified on other aircraft models, especially those with different empennage configurations.

Acknowledgments

This research was supported by the Federal Aviation Administration (FAA) Technical Center under Grant 93-G-026, Thomas DeFiore, Program Manager, and Terence Barnes, FAA National Resource Specialist for Flight Loads and Aeroelasticity.

References

- ¹Gabriel, E. A., DeFiore, T., Locke, J. E., and Smith, H. W., "General Aviation Aircraft-Normal Acceleration Data Analysis and Collection Project, Final Report," Dept. of Transportation, Rept. DOT/FAA/CT-91/20, Federal Aviation Administration, Washington, DC, 1993.
- ²"Fatigue Evaluation of Wing and Associated Structure on Small Airplanes," Federal Aviation Administration, Rept. AFS-120-73-2, Washington, DC, 1973.
- ³Van Gelder, P. A., "In-flight Tailload Measurements," *Proceedings of the 18th ICAS Congress*, AIAA, Washington, DC, 1992, pp. 1058-1066.
- ⁴Hoffman, M. E., "A Neural Network Prototype for Predicting F-14B Strains at the B.L.10 Longeron," NAWC, Rept. NAWCADWAR-92042-60, Warminster, PA, June 1992.
- ⁵Haas, J. D., Milano, J., and Flitter, L., "Prediction of Helicopter Component Loads Using Neural Networks," AIAA Paper 93-1301, April 1993.
- ⁶Cook, A. B., Fuller, C. R., O'Brien, W. F., and Cabell, R. H., "Artificial Neural Networks for Predicting Nonlinear Dynamic Helicopter Loads," *AIAA Journal*, Vol. 32, No. 5, 1994, pp. 1072-1074.
- ⁷Kim, D., and Marciniak, M., "Prediction of Vertical Tail Maneuver Loads Using Backpropagation Neural Networks," *Journal of Aircraft*, Vol. 37, No. 3, 2000, pp. 526-530.
- ⁸*A Technology Handbook for Professional II+ and NeuralWorks Explorer*, NeuralWare, Inc. Technical Publications Group, Pittsburgh, PA, 1995, pp. 235-237.
- ⁹MIL-HDBK-5E, Dept. of Defense, 1987.